Available online at www.sciencedirect.com
ScienceDirect
Journal of Solid State Chemistry 180 (2007) 2216–2224
JOURNAL OF SOLID STATE CHEMISTRY
www.elsevier.com/locate/jssc

Ternary rare-earth titanium antimonides: Phase equilibria in the *RE*–Ti–Sb (*RE* = La, Er) systems and crystal structures of $RE_2Ti_7Sb_{12}$ (*RE* = La, Ce, Pr, Nd) and $RETi_3(Sn_xSb_{1-x})_4$ (*RE* = Nd, Sm)

Haiying Bie[a], S.H. Devon Moore[a], Davin G. Piercey[a], Andriy V. Tkachuk[a], Oksana Ya. Zelinska[a,b], Arthur Mar[a,*]

[a]*Department of Chemistry, University of Alberta, Edmonton, Alta., Canada T6G 2G2*
[b]*Department of Inorganic Chemistry, Ivan Franko National University of Lviv, 79005 Lviv, Ukraine*

Received 1 April 2007; accepted 31 May 2007
Available online 6 June 2007

Abstract

Investigations on phase relationships and crystal structures have been conducted on several ternary rare-earth titanium antimonide systems. The isothermal cross-sections of the ternary *RE*–Ti–Sb systems containing a representative early (*RE* = La) and late rare-earth element (*RE* = Er) have been constructed at 800 °C. In the La–Ti–Sb system, the previously known compound La_3TiSb_5 was confirmed and the new compound $La_2Ti_7Sb_{12}$ (own type, *Cmmm*, $Z = 2$, $a = 10.5446(10)$ Å, $b = 20.768(2)$ Å, and $c = 4.4344(4)$ Å) was discovered. In the Er–Ti–Sb system, no ternary compounds were found. The structure of $La_2Ti_7Sb_{12}$ consists of a complex arrangement of $TiSb_6$ octahedra and disordered fragments of homoatomic Sb assemblies, generating a three-dimensional framework in which La atoms reside. Other early rare-earth elements (*RE* = Ce, Pr, Nd) can be substituted in this structure type. Attempts to prepare crystals in these systems through use of a tin flux resulted in the discovery of a new Sn-containing pseudoternary phase $RETi_3(Sn_xSb_{1-x})_4$ for *RE* = Nd, Sm (own type, *Fmmm*, $Z = 8$; $a = 5.7806(4)$ Å, $b = 10.0846(7)$ Å, and $c = 24.2260(16)$ Å for $NdTi_3(Sn_{0.1}Sb_{0.9})_4$; $a = 5.7590(4)$ Å, $b = 10.0686(6)$ Å, and $c = 24.1167(14)$ Å for $SmTi_3(Sn_{0.1}Sb_{0.9})_4$). Its structure consists of double-layer slabs of Ti-centred octahedra stacked alternately with nets of the *RE* atoms; the Ti atoms are arranged in kagome nets.
© 2007 Elsevier Inc. All rights reserved.

Keywords: Phase diagram; Crystal structure; Rare earths; Antimonide

1. Introduction

Ternary rare-earth transition-metal antimonides *RE*–*M*–Sb represent a rich and varied class of materials exhibiting diverse structures and physical properties [1]. Systems containing a late transition metal have been the focus of most previous studies, whereas those containing an early transition metal remain poorly investigated. When *M* is a group 4, 5, or 6 element, the only compounds known so far are RE_3MSb_5 (*M* = Ti, Zr, Hf, Nb) [2–5], $REMSb_3$ (*M* = V, Cr) [4–22], and *RE*ZrSb [23–26]. In the Sb-rich phases, homoatomic Sb bonding networks are a recurring feature of the structures, in the form of one-dimensional chains in RE_3MSb_5 or two-dimensional nets in $REMSb_3$. Given the absence of phase diagram information except for Dy–Zr–Sb (800 °C) [24], it is not clear if other compounds exist in these systems.

Systematic investigations on *RE*–Ti–Sb systems are presented here. The complete phase diagrams for a representative early (*RE* = La) and late rare earth (*RE* = Er) have been established at 800 °C. A new ternary phase, $RE_2Ti_7Sb_{12}$ (*RE* = La, Ce, Pr, Nd) has been identified and its structure determined. In addition, a pseudoternary phase, $RETi_3(Sn_xSb_{1-x})_4$ (*RE* = Nd, Sm) was discovered in the course of crystal growth experiments. Both of these phases adopt new structure types in which Ti-centred octahedra and homoatomic Ti–Ti or Sb–Sb bonding figure prominently.

*Corresponding author. Fax: +1 780 492 8231.
E-mail address: arthur.mar@ualberta.ca (A. Mar).

0022-4596/$ - see front matter © 2007 Elsevier Inc. All rights reserved.
doi:10.1016/j.jssc.2007.05.030

2. Experimental

2.1. Synthesis

The phase diagrams of the La–Ti–Sb and Er–Ti–Sb systems were investigated by arc melting of 80 and 50 alloys, respectively, which were prepared in an Edmund Bühler MAM-1 compact arc melter on a water-cooled copper block under an argon atmosphere gettered with Ti. Starting materials were pieces of the rare-earth elements (La, 99.9%, Hefa; Er, 99.9%, Cerac), Ti sponge (99.9%, Fisher), and Sb pieces (99.999%, Alfa-Aesar). The alloys were melted twice to ensure homogeneity. The final compositions of the alloys were determined with the assumption that the weight losses observed during arc melting (up to 5%) were attributed to volatilization of Sb alone. The alloys were then sealed in evacuated fused-silica tubes and annealed at 800 °C for 1 (Er–Ti–Sb) or 2 weeks (La–Ti–Sb). After the heat treatment, the tubes were quenched in cold water. Products were characterized by powder X-ray diffraction patterns collected on an Inel powder diffractometer equipped with a CPS 120 detector. Polished samples embedded in resin were examined by metallographic analyses. Approximate elemental compositions of phases were determined by energy-dispersive X-ray (EDX) analysis on a Hitachi S-2700 scanning electron microscope.

A new ternary phase found in the La–Ti–Sb system was initially believed to be the antimonide end-member analogue of the RETi$_3$(Sn$_x$Sb$_{1-x}$)$_4$ phase described below. To obtain crystals of this phase (subsequently identified as La$_2$Ti$_7$Sb$_{12}$), mixtures of La pieces (99.9%, Hefa), Ti powder (99.98%, Cerac), and Sb powder (99.995%, Cerac) in the molar ratio 1:3:4 were placed in an alumina crucible jacketed by an outer fused-silica tube. Under the optimum conditions for crystal growth, the evacuated tubes were heated to 650 °C over 1 d, heated to 1050 °C over 1 d, kept at that temperature for 2 d, slowly cooled to 800 °C over 4 d, kept at that temperature for 12 d, and then slowly cooled to 20 °C over 4 d. The major phase from these reactions was La$_3$TiSb$_5$ [2], which was difficult to distinguish from La$_2$Ti$_7$Sb$_{12}$ as all crystals obtained were small. Decreasing the reaction time or quenching from 800 °C tended to disfavour the formation of La$_2$Ti$_7$Sb$_{12}$ crystals.

Isostructural compounds RE_2Ti$_7$Sb$_{12}$ with RE = Ce, Pr, Nd were obtained (in combination with RE_3TiSb$_5$) by arc melting at the stoichiometric ratio of 2:7:12 and annealing at 900 °C over a relatively long time of 20 d. Use of different compositions near the target composition did not improve the phase purity substantially. Cell parameters are listed in Table 1.

The pseudoternary phase RETi$_3$(Sn$_x$Sb$_{1-x}$)$_4$ (RE = Nd, Sm) was first identified as a byproduct from a Sn-flux reaction intended to prepare crystals of RE_3TiSb$_5$ for physical property measurements [3]. A 0.25-g mixture of the elemental powders (Nd or Sm, 99.9%, Alfa-Aesar; Ti, 99.98%, Cerac; Sb, 99.998%, Aldrich) in the presence of a 10-fold weight excess of Sn (99.8%, Cerac) was placed in evacuated fused-silica tubes. Although crystals of the desired RE_3TiSb$_5$ phases were obtained from these reactions, EDX analyses revealed that some crystals consistently contained a small amount of Sn, with an Sn:Sb ratio of 1:9. Crystals of NdTi$_3$(Sn$_{0.1}$Sb$_{0.9}$)$_4$ were isolated from a reaction heated at 570 °C for 1 d and 950 °C for 2 d, followed by centrifuging to remove the Sn flux. Crystals of SmTi$_3$(Sn$_{0.1}$Sb$_{0.9}$)$_4$ were isolated from a reaction heated at 700 °C for 2 d, followed by centrifuging. Synthetic experiments in which different temperatures and different amounts of Sn were used did not improve the yields, although formation of the phase seems to be favoured at higher temperatures (>700 °C). Given that NdTi$_3$(Sn$_{0.1}$Sb$_{0.9}$)$_4$ and SmTi$_3$(Sn$_{0.1}$Sb$_{0.9}$)$_4$ were obtained in the presence of excess Sn, these formulas represent the upper limit of Sn solubility. The lower limit of Sn solubility in RETi$_3$(Sn$_x$Sb$_{1-x}$)$_4$ was not determined, but in light of our inability to prepare "RETi$_3$Sb$_4$" as described above, it is likely that this limit does not extend to $x = 0$. Further experiments to understand these synthetic difficulties are ongoing. For example, results from arc melting reactions with different loading compositions "SmTi$_3$(Sn$_x$Sb$_{1-x}$)$_4$" ($0 < x < 1$ in 0.1 increments) confirmed that this phase does not form beyond $x \geqslant 0.2$.

Table 1
Cell parameters for RE_2Ti$_7$Sb$_{12}$ (RE = La, Ce, Pr, Nd)[a]

Compound	a (Å)	b (Å)	c (Å)	V (Å^3)
La$_2$Ti$_7$Sb$_{12}$	10.5332(5)	20.733(1)	4.4338(2)	968.26(8)
Ce$_2$Ti$_7$Sb$_{12}$	10.497(1)	20.692(2)	4.4160(5)	959.1(2)
Pr$_2$Ti$_7$Sb$_{12}$	10.474(2)	20.689(4)	4.3896(9)	951.2(3)
Nd$_2$Ti$_7$Sb$_{12}$	10.427(2)	20.697(3)	4.3812(7)	945.5(3)

[a]Obtained from powder X-ray diffraction data.

2.2. Structure determination

Single-crystal X-ray diffraction data were collected on a Bruker Platform/SMART 1000 CCD diffractometer at 22 °C using ω scans. Structure solution and refinement were carried out with use of the SHELXTL (version 6.12) program package [27]. Face-indexed numerical absorption corrections were applied. Crystal data and further details of the data collection are given in Table 2.

For La$_2$Ti$_7$Sb$_{12}$, the intensity pattern indicated Laue symmetry and systematic extinctions consistent with the orthorhombic space groups *Cmmm*, *Cmm*2, and *C*222. Intensity statistics (mean $|E^2-1| = 0.946$) favoured the centrosymmetric space group *Cmmm*. Initial atomic positions for the La, Ti, and most of the Sb atoms in the structure were found by direct methods. The Sb2 and Sb3 sites exhibited elevated displacement parameters, suggesting partial occupancy. Two additional prominent peaks remaining in the difference electron density map were

Table 2
Crystallographic data for $La_2Ti_7Sb_{12}$ and $RETi_3(Sn_xSb_{1-x})_4$ (RE = Nd, Sm)

Formula	$La_2Ti_7Sb_{12}$	$NdTi_3(Sn_{0.1}Sb_{0.9})_4$	$SmTi_3(Sn_{0.1}Sb_{0.9})_4$
Formula mass (amu)	2074.12	773.72	779.83
Space group	*Cmmm* (No. 65)	*Fmmm* (No. 69)	*Fmmm* (No. 69)
a (Å)	10.5446(10)	5.7806(4)	5.7590(4)
b (Å)	20.768(2)	10.0846(7)	10.0686(6)
c (Å)	4.4344(4)	24.2260(16)	24.1167(14)
V (Å^3)	971.1(2)	1412.3(2)	1398.4(2)
Z	2	8	8
ρ_{calcd} (g cm^{-3})	7.093	7.278	7.408
Crystal dimensions (mm)	$0.08 \times 0.05 \times 0.04$	$0.23 \times 0.20 \times 0.10$	$0.19 \times 0.06 \times 0.03$
Radiation	Graphite monochromated Mo$K\alpha$, $\lambda = 0.71073$ Å		
μ (Mo$K\alpha$) (cm^{-1})	233.26	252.40	264.62
Transmission factors	0.176–0.454	0.027–0.130	0.114–0.460
2θ limits	$3.92^\circ \leqslant 2\theta$ (Mo$K\alpha$) $\leqslant 66.32^\circ$	$3.36^\circ \leqslant 2\theta$ (Mo$K\alpha$) $\leqslant 65.16^\circ$	$6.76^\circ \leqslant 2\theta$ (Mo$K\alpha$) $\leqslant 65.10^\circ$
Data collected	$-15 \leqslant h \leqslant 15$, $-31 \leqslant k \leqslant 31$, $-6 \leqslant l \leqslant 6$	$-8 \leqslant h \leqslant 8$, $-15 \leqslant k \leqslant 15$, $-36 \leqslant l \leqslant 36$	$-8 \leqslant h \leqslant 8$, $-15 \leqslant k \leqslant 14$, $-33 \leqslant l \leqslant 36$
No. of data collected	6703	3499	3531
No. of unique data, including $F_o^2 < 0$	1083 ($R_{int} = 0.058$)	742 ($R_{int} = 0.033$)	732 ($R_{int} = 0.030$)
No. of unique data, with $F_o^2 > 2\sigma(F_o^2)$	889	742	712
No. of variables	52	29	29
$R(F)$ for $F_o^2 > 2\sigma(F_o^2)$[a]	0.040	0.021	0.025
$R_w(F_o^2)$[b]	0.100	0.049	0.060
Goodness-of-fit	1.064	1.341	1.281
$(\Delta\rho)_{max}$, $(\Delta\rho)_{min}$ (e Å^{-3})	3.01, −3.21	1.75, −2.98	2.01, −2.60

[a] $R(F) = \frac{\sum ||F_o| - |F_c||}{\sum |F_o|}$.

[b] $R_w(F_o^2) = \geqslant \left[\frac{\sum [w(F_o^2 - F_c^2)^2]}{\sum wF_o^4}\right]^{1/2}$; $w^{-1} = \sigma^2(F_o^2) + (Ap)^2 + Bp$, where $p = \frac{\max(F_o^2, 0) + 2F_c^2}{3}$.

assigned as partially occupied Sb5 and Sb6 sites. When allowed to refine freely, the occupancies of these sites converged to 0.50(1) for Sb2, 0.50(1) for Sb3, 0.21(1) for Sb5, and 0.19(1) for Sb6. The occupancies of these sites (Sb2/Sb6 and Sb3/Sb5) are correlated because of chemically impossible short distances between them and symmetry-equivalent positions, and are limited to a maximum of 0.50 for Sb2 and Sb3, and 0.25 for Sb5 and Sb6. All other sites were essentially fully occupied (0.97(1)–1.06(1)), except for Ti3, whose occupancy converged to 0.85(2). The Sb1 site exhibits an elongated displacement parameter, which could be resolved into two very closely separated split sites (<0.4 Å), each half-occupied. If all these partial occupancies are taken at face value, the resulting formula is "$La_2Ti_{6.8}Sb_{11.8}$". Other orthorhombic space groups in which one or more mirror planes are removed (*Cmm*2, *C*222, and their permutations) as well as lower-symmetry monoclinic space groups (*C*2/*m*, *Cm*) were considered, including the possibility for twinning, but these failed to lead to ordered structural models. To arrive at a simple model for a local interpretation of the disorder implied by the partially occupied Sb sites, we have retained the structure in *Cmmm* but with the occupancies fixed at 0.50 for Sb2 and Sb3, 0.25 for Sb5 and Sb6, and 1.00 for all remaining atoms, and with the Sb1 site unsplit. This model thus neglects the slight substoichiometry inherent in the Sb5, Sb6, and Ti3 sites. The formula corresponding to this simplified structural model is "$La_2Ti_7Sb_{12}$" and will be referred to as such in the remaining discussion.

For $RETi_3(Sn_xSb_{1-x})_4$ (RE = Nd, Sm), preliminary Weissenberg photography gave initial cell parameters, and revealed Laue symmetry and systematic extinctions consistent with the orthorhombic space groups *Fmmm*, *Fmm*2, and *F*222. Intensity statistics (mean $|E^2-1| = 0.940$, 0.944 for RE = Nd, Sm, respectively) favoured the centrosymmetric space group *Fmmm*. Initial positions for all atoms in the structure were readily found by direct methods. Refinements proceeded in a straightforward manner with reasonable displacement parameters and full occupancies found for all sites. Because Sn and Sb cannot be distinguished on the basis of their similar scattering factors, they were assumed to be distributed randomly over each of the three sites found, with occupancies fixed to reflect the ratio determined from EDX analysis (0.1 Sn/0.9 Sb). The formula thus corresponds to $RETi_3(Sn_{0.1}Sb_{0.9})_4$.

Atomic positions were standardized with the program STRUCTURE TIDY [28]. Final values of the positional and displacement parameters are given in Table 3. Selected interatomic distances are listed in Tables 4 and 5. Further data, in CIF format, have been sent to Fachinformationszentrum Karlsruhe, Abt. PROKA, 76344 Eggenstein-Leopoldshafen, Germany, as supplementary material No. CSD-418173 ($La_2Ti_7Sb_{12}$), 418174 ($NdTi_3(Sn_{0.1}Sb_{0.9})_4$), and 418175 ($SmTi_3(Sn_{0.1}Sb_{0.9})_4$), and can be obtained by

Table 3
Atomic coordinates and equivalent isotropic displacement parameters for $La_2Ti_7Sb_{12}$ and $RETi_3(Sn_xSb_{1-x})_4$ (RE = Nd, Sm)

Atom	Wyckoff position	Occupancy	x	y	z	U_{eq} (Å^2)[a]
$La_2Ti_7Sb_{12}$						
La	4*i*	1	0	0.38857(4)	0	0.0087(2)
Ti1	8*p*	1	0.1451(2)	0.11989(9)	0	0.0136(4)
Ti2	4*e*	1	1/4	1/4	0	0.0103(4)
Ti3	2*a*	1	0	0	0	0.0167(7)
Sb1	8*q*	1	0.29146(9)	0.16415(5)	1/2	0.025(2)
Sb2	8*o*	0.50	0.2596(1)	0	0.1173(3)	0.0135(3)
Sb3	8*n*	0.50	0	0.22999(6)	0.1373(3)	0.0080(2)
Sb4	4*j*	1	0	0.08027(5)	1/2	0.0150(2)
Sb5	4*j*	0.25	0	0.2208(3)	1/2	0.033(1)
Sb6	4*h*	0.25	0.2328(6)	0	1/2	0.037(1)
Sb7	2*c*	1	1/2	0	1/2	0.013(3)
$NdTi_3(Sn_{0.1}Sb_{0.9})_4$						
Nd	8*i*	1	0	0	0.30482(2)	0.0051(1)
Ti1	16*j*	1	1/4	1/4	0.09540(3)	0.0041(2)
Ti2	8*i*	1	0	0	0.09205(5)	0.0048(2)
Sn1/Sb1	16*m*	0.1/0.9	0	0.16045(3)	0.18773(1)	0.0050(1)
Sn2/Sb2	8*i*	0.1/0.9	0	0	0.43425(2)	0.0052(1)
Sn3/Sb3	8*h*	0.1/0.9	0	0.17078(4)	0	0.0060(1)
$SmTi_3(Sn_{0.1}Sb_{0.9})_4$						
Sm	8*i*	1	0	0	0.30473(2)	0.0073(1)
Ti1	16*j*	1	1/4	1/4	0.09597(4)	0.0058(2)
Ti2	8*i*	1	0	0	0.09236(6)	0.0065(3)
Sn1/Sb1	16*m*	0.1/0.9	0	0.15981(3)	0.18876(2)	0.0069(1)
Sn2/Sb2	8*i*	0.1/0.9	0	0	0.43362(2)	0.0071(1)
Sn3/Sb3	8*h*	0.1/0.9	0	0.17097(5)	0	0.0078(1)

[a] U_{eq} is defined as one-third of the trace of the orthogonalized U_{ij} tensor.

Table 4
Selected interatomic distances (Å) in $La_2Ti_7Sb_{12}$

La–Sb7 (× 2)	3.2050(6)	Sb1–Sb5	3.247(5)
La–Sb1 (× 4)	3.3091(7)	Sb1–Sb5	3.291(2)
La–Sb3	3.349(1)	Sb1–Sb6	3.465(3)
La–Sb2 (× 2)	3.471(1)	Sb2–Sb6	2.752(2)
Ti1–Sb2	2.816(2)	Sb2–Sb7	3.050(1)
Ti1–Sb4 (× 2)	2.816(1)	Sb2–Sb2	3.394(3)
Ti1–Sb3	2.818(2)	Sb2–Sb7	3.731(3)
Ti1–Sb1 (× 2)	2.854(1)	Sb3–Sb5	2.833(1)
Ti2–Sb3 (× 2)	2.7373(4)	Sb3–Sb3	3.216(3)
Ti2–Sb1 (× 4)	2.8785(6)	Sb4–Sb5	2.918(6)
Ti3–Sb4 (× 4)	2.7740(6)	Sb4–Sb6	2.968(5)
Ti3–Sb2 (× 2)	2.787(1)	Sb4–Sb4	3.334(3)
Ti1–Ti2	2.920(2)	Sb6–Sb7	2.817(6)
Ti1–Ti3	2.922(2)		
Ti1–Ti1	3.059(4)		

Table 5
Selected interatomic distances (Å) in $RETi_3(Sn_xSb_{1-x})_4$ (RE = Nd, Sm)[a]

	$NdTi_3(Sn_{0.1}Sb_{0.9})_4$	$SmTi_3(Sn_{0.1}Sb_{0.9})_4$
RE–*X*2	3.1357(6)	3.1084(7)
RE–*X*1 (× 2)	3.2656(5)	3.2266(6)
RE–*X*1 (× 4)	3.3173(2)	3.3023(2)
RE–*X*1 (× 2)	3.4290(4)	3.4288(4)
Ti1–*X*1 (× 2)	2.8118(7)	2.8115(8)
Ti1–*X*3 (× 2)	2.8405(7)	2.8396(8)
Ti1–*X*2 (× 2)	2.9934(3)	2.9863(3)
Ti2–*X*3 (× 2)	2.8176(10)	2.8151(12)
Ti2–*X*1 (× 2)	2.8268(11)	2.8272(13)
Ti2–*X*2 (× 2)	2.9597(3)	2.9469(4)
Ti1–Ti1	2.8903(2)	2.8795(2)
Ti1–Ti2	2.9071(2)	2.9011(2)
*X*1–*X*1	3.2361(6)	3.2181(7)
*X*1–*X*1	3.4082(4)	3.4044(4)
*X*1–*X*1	3.5165(7)	3.4676(8)
*X*2–*X*2	3.1857(9)	3.2019(11)
*X*3–*X*3	3.3025(5)	3.2901(5)
*X*3–*X*3	3.4445(9)	3.4428(10)

[a] *X* represents the disordered sites containing 0.1 Sn and 0.9 Sb.

contacting FIZ (quoting the article details and the corresponding CSD numbers).

3. Results and discussion

3.1. Phase diagrams

Apart from the existence of RE_3TiSb_5 (RE = La, Ce, Pr, Nd, Sm) phases, which were first discovered in Sn-flux reactions [2], little else is known about the ternary *RE*–Ti–Sb systems. The termination of the RE_3TiSb_5 series at RE = Sm suggests that the phase behaviour will differ for early vs. late *RE* elements. For this reason, a representative early and late *RE* member was chosen for more comprehensive phase diagram investigations. Fig. 1

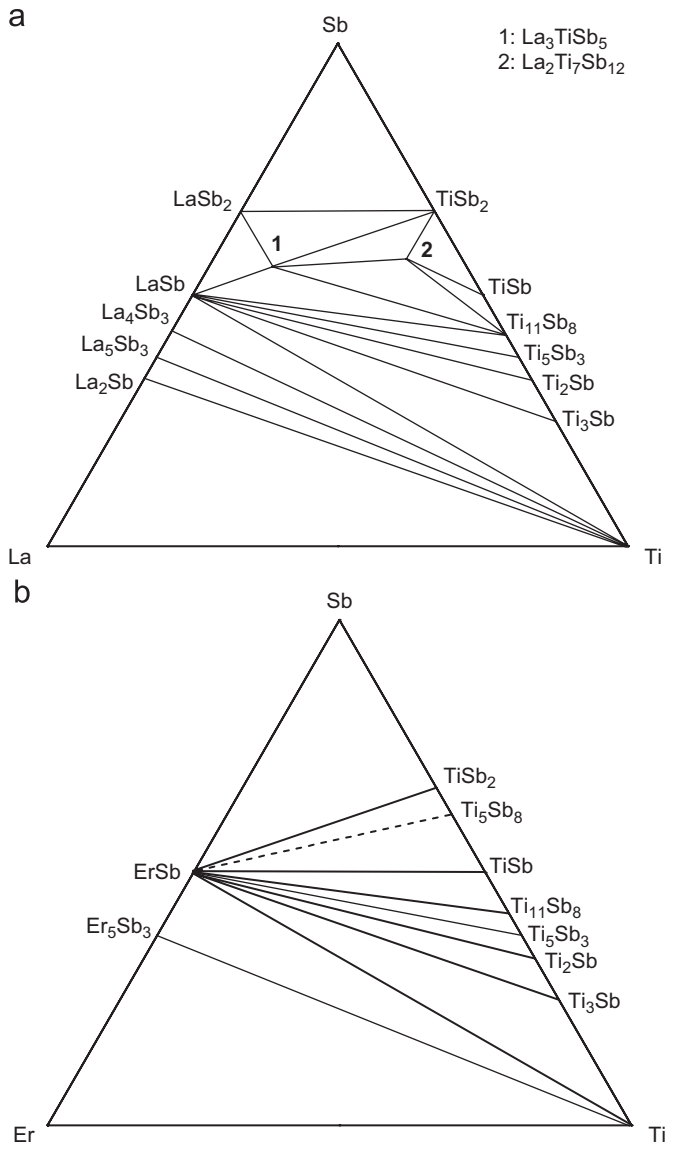

Fig. 1. Isothermal sections at 800 °C of the (a) La–Ti–Sb and (b) Er–Ti–Sb phase diagrams.

shows the isothermal sections at 800 °C of the La–Ti–Sb and Er–Ti–Sb systems. At this temperature, previous information suggests that liquid forms in the region above 95 at% Sb [29], so highly antimony-rich compositions (>70 at% Sb) in the ternary phase diagrams were not examined.

In the *RE*–Sb sections of both systems, all previously known binary phases were observed except for Er_4Sb_3 [30] and the high-pressure phase $ErSb_2$ [31]. In the Ti–Sb sections of both systems, the existence of six binary phases was confirmed: cubic Ti_3Sb [32], Ti_2Sb [33], Ti_5Sb_3 [34,35], $Ti_{11}Sb_8$ [36], TiSb [32], and $TiSb_2$ [37]. The solubility of the *RE* component in these binary Ti–Sb phases was established to be less than 1 at%. The phases Ti_2Sb and $Ti_{11}Sb_8$ were reported recently [33,36]. Other phases (Ti_4Sb, $Ti_{2.5}Sb$, and Ti_6Sb_5) reported in earlier investigations were not observed under the conditions used here. Ti_4Sb was initially formulated as "$Ti_3(Ti_{0.2}Sb_{0.8})$" [38] but later attempts to reproduce its synthesis by arc melting failed [32], so perhaps it is a metastable phase. $Ti_{2.5}Sb$ was originally prepared in carbon crucibles and heated in a high-pressure furnace or an induction furnace [39], but neither arc melting nor heating at 1400–1600 °C yielded this phase [32]. The existence of $Ti_{2.5}Sb$ can also be discounted, on the basis of the stability of Ti_2Sb with respect to disproportionation to Ti_3Sb and Ti_5Sb_3 [33]. Ti_6Sb_5 was originally prepared by arc melting but its structure was unknown [32]; it is probably the phase now identified as $Ti_{11}Sb_8$ [36], given the similarity of their cell constants and powder X-ray diffraction patterns. Within the Er–Ti–Sb phase diagram, formation of the phase Ti_5Sb_8 [40] was sometimes observed in combination with TiSb and $TiSb_2$ at 800 °C in the 50–67 at% Sb region. When the annealing temperature was raised to 1000 °C, the expected equilibrium mixture of Ti_5Sb_8 with one of TiSb or $TiSb_2$ was formed. Ti_5Sb_8 has been indicated previously to be stable with respect to disproportionation (to TiSb and $TiSb_2$) between 900 and 1100 °C [40]. The non-equilibrium formation of Ti_5Sb_8 suggests that the annealing time of 1 week in the Er–Ti–Sb phase investigation may not have been sufficiently long. Although the structures of several mixed-metal representatives $(M',Ti)_5Sb_8$ (M' = Zr, Hf, Nb, Mo) are known [41], crystallographic details for the end-member Ti_5Sb_8 itself have not been reported previously [40]. Cell parameters obtained here from a single-crystal X-ray structure determination on tetragonal Ti_5Sb_8 are $a = 6.492(4)$ Å, $c = 26.514(15)$ Å, and $V = 1117.3(18)$ Å^3 [42].

In the Er–Ti–Sb system, no ternary compounds were found at 800 °C. In the La–Ti–Sb system, in addition to the previously known phase La_3TiSb_5 [2], the new compound $La_2Ti_7Sb_{12}$ was discovered, as revealed by EDX analyses of polished samples and by a hitherto unidentified powder X-ray diffraction pattern of ground samples.

3.2. Structure of $RE_2Ti_7Sb_{12}$

The compounds $RE_2Ti_7Sb_{12}$ (*RE* = La, Ce, Pr, Nd) adopt a new structure type. The structure of $La_2Ti_7Sb_{12}$ projected down the *c* direction is shown in Fig. 2. It consists of a complex three-dimensional framework of linked $TiSb_6$ octahedra. The Sb2 and Sb3 sites each have an occupancy of 0.50, but to clarify the presence of these $TiSb_6$ octahedra, the figure portrays one possible idealized model in which half of these sites are occupied in an ordered fashion and the other half are not shown. Three types of Ti-centred octahedra are then evident, each forming infinite chains through edge-sharing with their symmetry equivalents along the *c* direction. They differ in their connectivity along the *a* direction: The Ti1-centred octahedra are connected in pairs by sharing a common face (Sb4–Sb4–Sb3), the Ti2-centred octahedra are connected to form zigzag chains through corner-sharing of *trans* Sb3 atoms, and the Ti3-centred octahedra remain isolated.

Lastly, the Ti1-, Ti2-, and Ti3-centred octahedra are connected by face-sharing along the [1 1 0] and [1 $\bar{1}$ 0] directions. The Ti–Sb distances range from 2.7373(4) to 2.8785(6) Å, the shortest being similar to the sum of the Pauling radii ($r_{Ti} + r_{Sb} = 1.324 + 1.391 = 2.715$ Å) [43] and the longest being similar to those found in $TiSb_6$ octahedra in TiSb (2.846 Å) [32] and La_3TiSb_5 (2.859(1) Å) [2]. The occurrence of face-sharing octahedra brings the Ti centres in close contact with each other, at distances (2.920(2)–3.059(4) Å) that may be indicative of weak metal–metal bonding.

The network of $TiSb_6$ octahedra outlines channels that are occupied by the La and Sb7 atoms. The coordination geometry of Sb atoms around the La centres is approximately tricapped trigonal prismatic, corresponding to CN9 (4 Sb1, 2 Sb7, 0.50×4 Sb2, 0.50×2 Sb3), with La–Sb distances of 3.2050(6)–3.471(1) Å. Surrounding Sb7 in a distorted planar environment are four Sb2 atoms (with the half occupancy of the Sb2 sites taken into account), two that are within weak Sb–Sb bonding distances (3.050(1) Å) and two that are too far to be bonding (3.731(3) Å), on average.

Close to the half-occupied Sb2 and Sb3 sites are two other sites, Sb5 and Sb6, each having an occupancy of 0.25. These partially occupied Sb sites correspond to a complicated disorder. Fig. 3 shows one possible local interpretation for this disorder within a chain of edge-sharing Ti1-centred octahedra extending along the *c* direction. Full occupation of these sites is clearly precluded by the impossibly short Sb–Sb distances that would result.

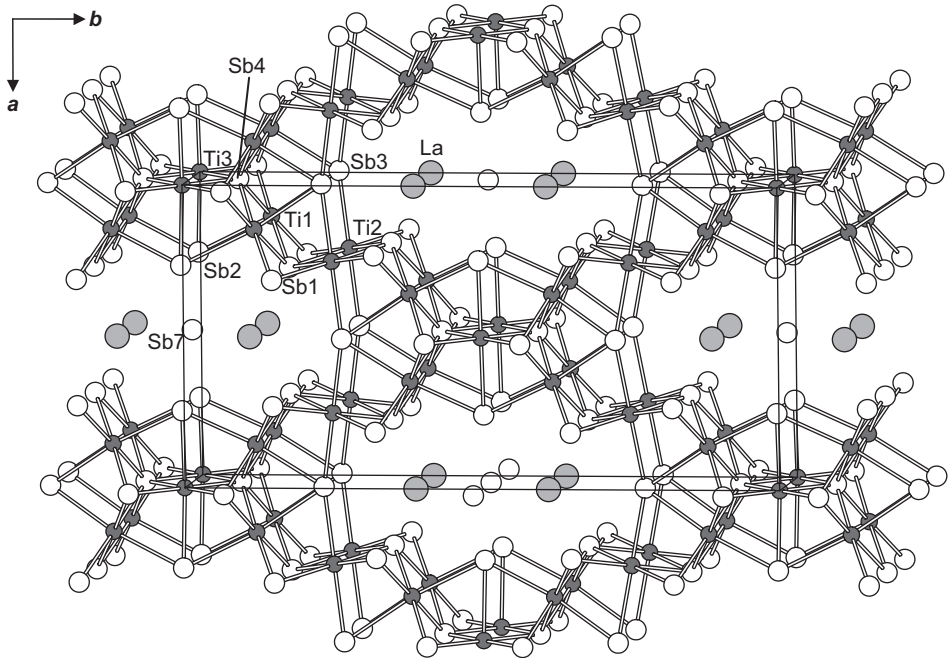

Fig. 2. Structure of $La_2Ti_7Sb_{12}$ viewed down the *c* direction. The large lightly shaded circles are La atoms, the small solid circles are Ti atoms, and the medium open circles are Sb atoms.

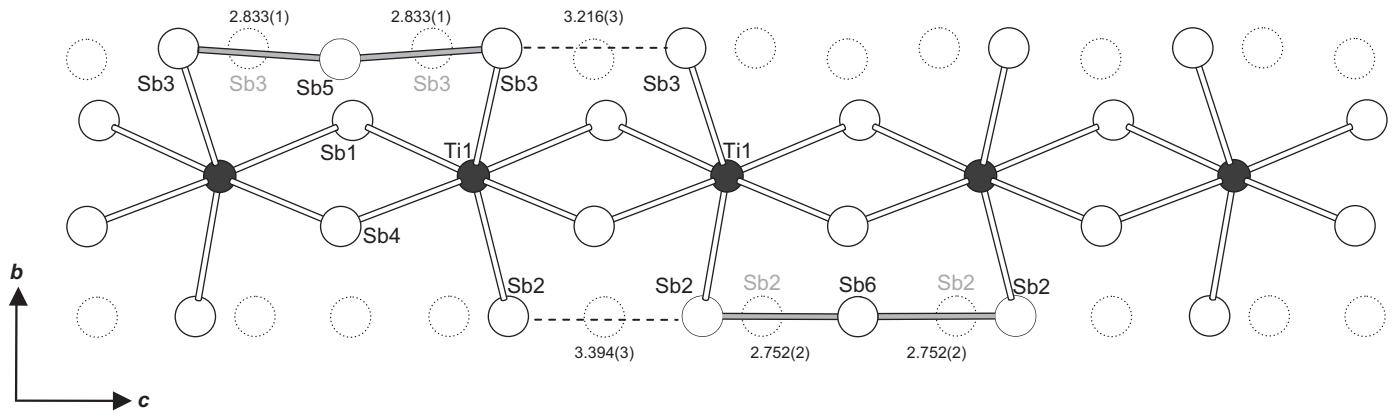

Fig. 3. One possible local ordering of the partially occupied Sb sites (0.50 for Sb2 and Sb3; 0.25 for Sb5 and Sb6) within an edge-sharing chain of Ti1-centred octahedra extended along the *c* direction in $La_2Ti_7Sb_{12}$.

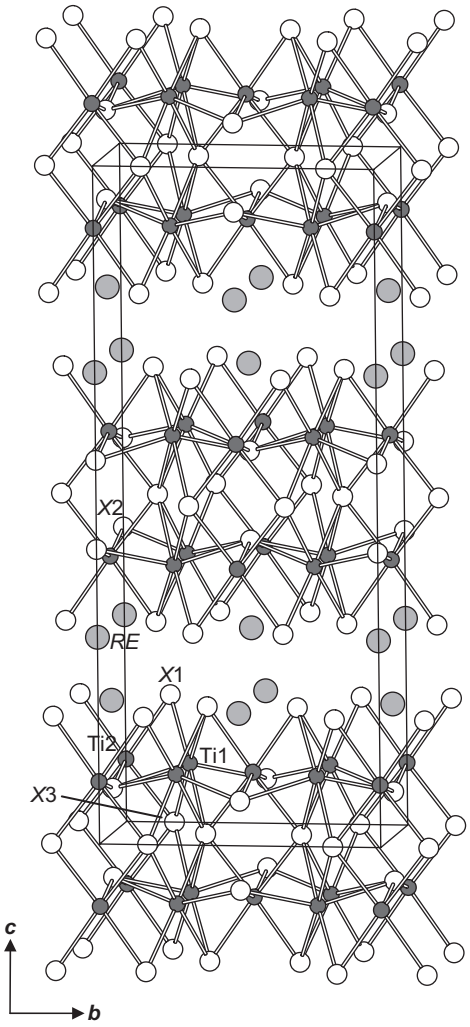

Fig. 4. Structure of $NdTi_3(Sn_{0.1}Sb_{0.9})_4$ or $SmTi_3(Sn_{0.1}Sb_{0.9})_4$ viewed down the *a* direction. The large lightly shaded circles are RE = Nd or Sm atoms, the small solid circles are Ti atoms, and the medium open circles are X = Sn or Sb atoms.

However, the level of partial occupancy is understandable on the basis that a minimum Sb–Sb distance cannot be less than ~2.7 Å. Distances of 2.8–2.9 Å are indicative of Sb–Sb single bonds, whereas longer distances of ~3.0–3.2 Å typically suggest hypervalent Sb–Sb bonds, although longer values have been implicated as non-innocent [44]. Within this edge-sharing octahedral chain, the apices are formed by the Sb2 and Sb3 sites; fixing their occupancy at 0.50 maintains CN6 around the Ti1 centres. An Sb5 atom must then lie between a pair of Sb3 atoms, and an Sb6 atom between a pair of Sb2 atoms, forming linear trimers containing rather short Sb–Sb contacts (Sb3–Sb5, 2.833(1) Å; Sb2–Sb6, 2.752(2) Å). These short distances are likely a result of matrix effects, analogous to the situation in $Ti_{11}Sb_8$ where similar Sb–Sb distances of 2.759(2) Å are found in linear Sb chains [36]. Even if long-range ordering of these trimers ensues within an individual edge-sharing octahedral chain, this ordering need not be in registry between different chains, leading to the observed average disordered structure.

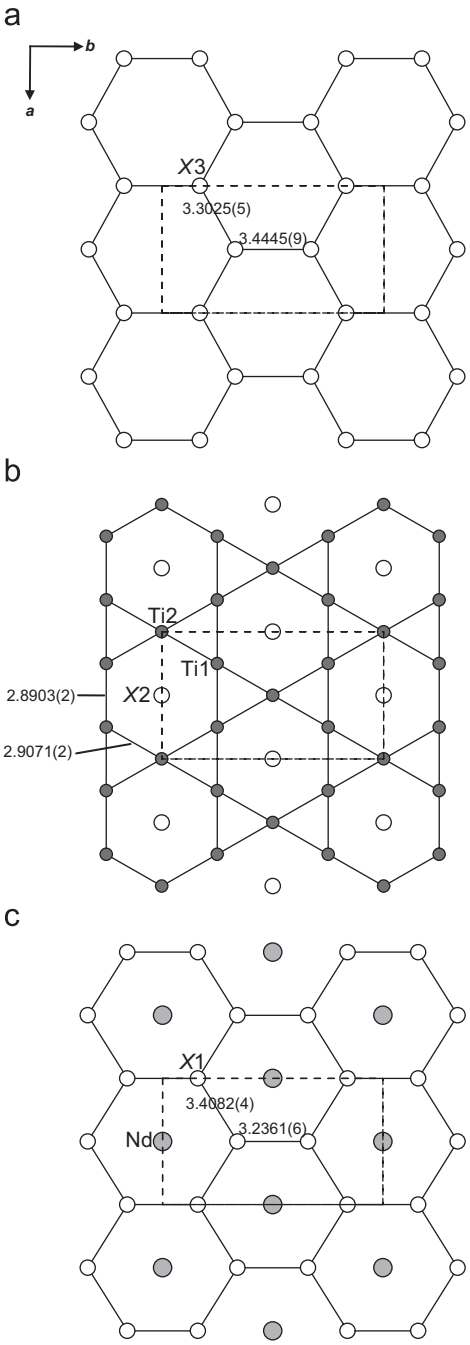

Fig. 5. Structure of $NdTi_3(Sn_{0.1}Sb_{0.9})_4$ in terms of nets: (a) 6^3 net of $X3$ atoms, (b) 3636 (kagome) net of Ti atoms with hexagons centred by $X2$ atoms, and (c) 6^3 net of $X1$ atoms with hexagons centred by Nd atoms.

3.3. Structure of $RETi(Sn_xSb_{1-x})_4$

The structures adopted by the pseudoternary compounds $RETi_3(Sn_{0.1}Sb_{0.9})_4$ (RE = Nd, Sm) are also new. To facilitate discussion, we focus on the Nd member and introduce the label X to denote the disordered Sn/Sb sites. The structure of $NdTi_3(Sn_{0.1}Sb_{0.9})_4$ projected down the *a* direction is shown in Fig. 4. It consists of two-dimensional slabs of linked $TiSb_6$ octahedra, stacked alternately with two-layer nets of Nd atoms along the *c* direction.

Extending along the *a* direction are two types of infinite chains, one formed by face sharing of Ti1-centred octahedra and one formed by corner sharing of Ti2-centred octahedra. Alternate chains are connected along the *b* direction through face sharing to form infinite layers parallel to the *ab* plane. Two such layers are then connected by edge sharing of octahedra along the *c* direction to form the slabs. The Ti–*X* distances of 2.8118(7)–2.9934(3) Å here are slightly longer than the Ti–Sb distances in $La_2Ti_7Sb_{12}$. Surrounding each Nd centre are six coplanar *X* atoms, plus one above and two below, resulting in a nine-coordinate geometry with Nd–*X* distances of 3.1357(6)–3.4290(4) Å. The shortest distance between *X* atoms is the *X*2–*X*2 contact of 3.1857(9) Å, corresponding to a dumbbell oriented along the *c* direction within the two-layer slab.

The structures of many intermetallic compounds can also be often conveniently described in terms of a stacking of nets [45], and $NdTi_3(Sn_{0.1}Sb_{0.9})_4$ is no exception. Each slab can be constructed from a stacking of five nets. The nets are of three types, as shown in Fig. 5. The central net is a simple hexagonal arrangement of *X*3 atoms, called a 6^3 net in Schläfli notation [45]. Above it is a kagome, or 6363 net, built up of Ti1 and Ti2 atoms, with the hexagons centred by *X*2 atoms. On top is a 6^3 net of *X*1 atoms with the hexagons centred by Nd atoms. The central net of *X*3 atoms lies on a mirror plane, across which reflection generates symmetry equivalents of the two other nets and thus the five-net-thick slab. The slabs alternate in disposition in an AB sequence as they are stacked along the *c* direction. Within the kagome net of Ti atoms, extensive Ti–Ti bonding is suggested by the 2.8903(2)–2.9071(2) Å distances.

3.4. Structural relationships and bonding

Although not evident at first inspection, the structures of $La_2Ti_7Sb_{12}$ and $NdTi_3(Sn_xSb_{1-x})_4$ show interesting relationships to each other. We focus on sectioned layers consisting of linked Ti-centred octahedra. In $NdTi_3(Sn_xSb_{1-x})_4$, such a layer consists of alternating, perfectly linear chains of corner-sharing and of face-sharing octahedra, extended along the *a* direction (Fig. 6a). Proceeding to $La_2Ti_7Sb_{12}$, the layer is derived by removing every second Ti centre from half of the chains of corner-sharing octahedra and every third and fourth one from all the chains of face-sharing octahedra (Fig. 6b). Thus, the layer in $La_2Ti_7Sb_{12}$ may be regarded as a defect variant of that in $NdTi_3(Sn_xSb_{1-x})_4$. The corner-sharing octahedral chains are no longer perfectly linear but adopt a zigzag configuration. Moreover, the cavity that is formed by removal of some of the corner-sharing octahedra is occupied by new Sb atoms. The shortest Ti–Ti interactions in these structures are associated with occurrence of the face-sharing octahedra, when Ti centres can approach each other most closely, by geometrical arguments. An alternative possibility of a defect structure is to remove all the corner-sharing octahedra, which results in isolated chains of only face-sharing octahedra, as occurs in the hexagonal structure of La_3TiSb_5 (Fig. 6c).

Bonding in these complex disordered structures is not easy to rationalize. For $NdTi_3(Sn_xSb_{1-x})_4$, we can consider the hypothetical antimonide end-member "$NdTi_3Sb_4$". If Sb–Sb interactions are assumed to be absent (because the contacts of 3.2 Å or greater are rather long) and Nd is assumed to be trivalent, then charge balance requires that the Ti atoms will have a partly filled *d* configuration, $(Nd^{3+})(Ti^{3+})_3(Sb^{3-})_4$, consistent with the occurrence of Ti–Ti distances (~2.9 Å) that may indicate metal–metal bonding. Introduction of a small amount of Sn into the Sb sites does not change this conclusion. For $La_2Ti_7Sb_{12}$, the situation is even more complicated, since both Ti–Ti (2.9–3.0 Å) and Sb–Sb bonding (2.8–3.2 Å) are probably operative. If no Ti–Ti bonding is assumed, then compliance with a charge-balanced formula $(La^{3+})_2(Ti^{4+})_7(Sb^{2.8-})_{12}$

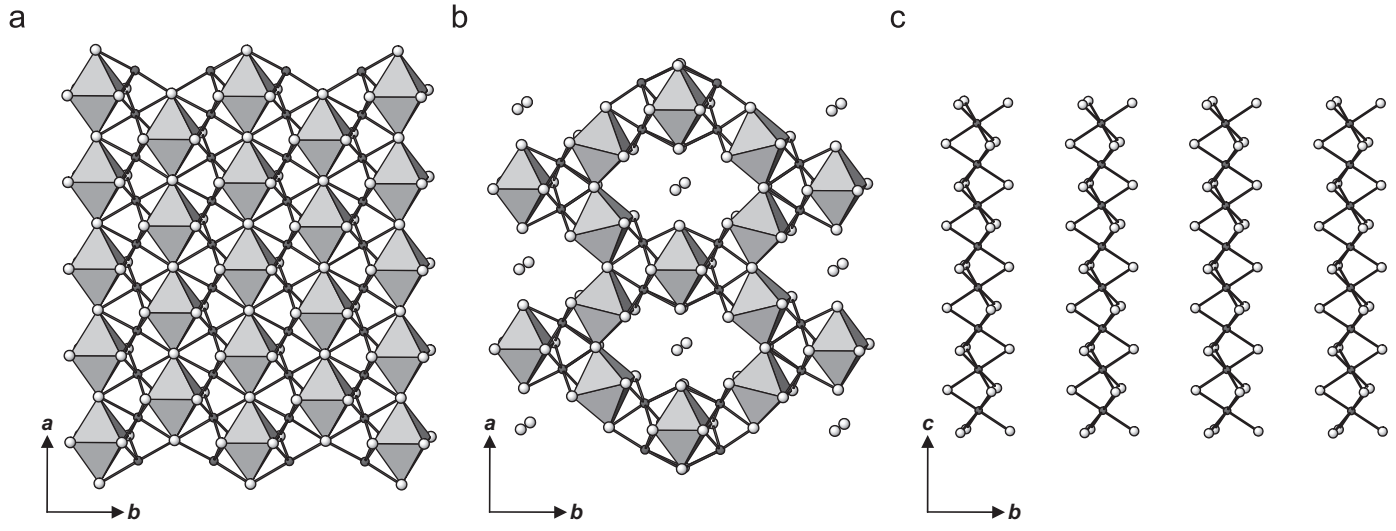

Fig. 6. Comparison of the structures of (a) $NdTi_3(Sn_xSb_{1-x})_4$, (b) $La_2Ti_7Sb_{12}$, and (c) La_3TiSb_5. Face-sharing Ti-centred octahedra are shown as ball-and-stick representations, and corner-sharing (or isolated) octahedra as polyhedral representations.

leads to the conclusion that some Sb–Sb bonding must be present. Conversely, if no Sb–Sb bonding is assumed, then the impossible formula $(La^{3+})_2(Ti^{4.3+})_7(Sb^{3-})_{12}$ leads by *reductio ad absurdum* to the same conclusion.

The present work has revealed new phases among the *RE*–Ti–Sb systems adopting complex crystal structures. The range of *RE* substitution is limited to the early *RE* elements in $RE_2Ti_7Sb_{12}$ (RE = La, Ce, Pr, Nd) and $RETi_3(Sn_xSb_{1-x})_4$ (RE = Nd, Sm). Although the Er–Ti–Sb system was found to contain no ternary phases, it may be worthwhile investigating systems containing other late *RE* elements, such as Yb, whose propensity for divalency may lead to different phase behaviour.

Acknowledgments

The Natural Sciences and Engineering Research Council of Canada and the University of Alberta supported this work. We thank Dr. Robert McDonald and Dr. Michael J. Ferguson (X-ray Crystallography Laboratory) for the X-ray data collection and Ms. Christina Barker (Department of Chemical and Materials Engineering) for assistance with the EDX analysis.

References

[1] O.L. Sologub, P.S. Salamakha, in: K.A. Gschneidner Jr., J.-C.G. Bünzli, V.K. Pecharsky (Eds.), Handbook on the Physics and Chemistry of Rare Earths, vol. 33, Elsevier, Amsterdam, 2003, pp. 35–146.
[2] G. Bolloré, M.J. Ferguson, R.W. Hushagen, A. Mar, Chem. Mater. 7 (1995) 2229–2231.
[3] S.H.D. Moore, L. Deakin, M.J. Ferguson, A. Mar, Chem. Mater. 14 (2002) 4867–4873.
[4] A.V. Tkachuk, S.J. Crerar, X. Wu, C.P.T. Muirhead, L. Deakin, A. Mar, Mater. Res. Soc. Symp. Proc. 848 (2005) 75–82.
[5] M.J. Ferguson, R.W. Hushagen, A. Mar, J. Alloys Compd. 249 (1997) 191–198.
[6] M. Brylak, W. Jeitschko, Z. Naturforsch. B: Chem. Sci. 50 (1995) 899–904.
[7] K. Hartjes, W. Jeitschko, M. Brylak, J. Magn. Magn. Mater. 173 (1997) 109–116.
[8] N.P. Raju, J.E. Greedan, M.J. Ferguson, A. Mar, Chem. Mater. 10 (1998) 3630–3635.
[9] M. Leonard, S. Saha, N. Ali, J. Appl. Phys. 85 (1999) 4759–4761.
[10] M.L. Leonard, I.S. Dubenko, N. Ali, J. Alloys Compd. 303/304 (2000) 265–269.
[11] I.S. Dubenko, P. Hill, N. Ali, J. Appl. Phys. 89 (2001) 7326–7328.
[12] D.D. Jackson, M. Torelli, Z. Fisk, Phys. Rev. B 65 (2001) 014421-1–014421-7.
[13] E. Granado, H. Martinho, M.S. Sercheli, P.G. Pagliuso, D.D. Jackson, M. Torelli, J.W. Lynn, C. Rettori, Z. Fisk, S.B. Oseroff, Phys. Rev. Lett. 89 (2002) 107204-1–107204-4.
[14] J.H. Shim, B.I. Min, J. Magn. Magn. Mater. 272–276 (2004) e241–e242.
[15] M. Richter, J. Rusz, H. Rosner, K. Koepernik, I. Opahle, U. Nitzsche, H. Eschrig, J. Magn. Magn. Mater. 272–276 (2004) e251–e252.
[16] L. Deakin, M.J. Ferguson, A. Mar, J.E. Greedan, A.S. Wills, Chem. Mater. 13 (2001) 1407–1412.
[17] D.D. Jackson, Z. Fisk, J. Magn. Magn. Mater. 256 (2003) 106–116.
[18] L. Deakin, A. Mar, Chem. Mater. 15 (2003) 3343–3346.
[19] D.D. Jackson, Z. Fisk, J. Alloys Compd. 377 (2004) 243–247.
[20] S.J. Crerar, L. Deakin, A. Mar, Chem. Mater. 17 (2005) 2780–2784.
[21] D.D. Jackson, Z. Fisk, Phys. Rev. B 73 (2006) 024421/1–024421/7.
[22] W.A. MacFarlane, K.H. Chow, Z. Salman, A.V. Tkachuk, A. Mar, Physica B 374/375 (2006) 71–74.
[23] A.V. Morozkin, I.A. Sviridov, J. Alloys Compd. 320 (2001) L1–L2.
[24] A.V. Morozkin, I.A. Sviridov, A.V. Leonov, J. Alloys Compd. 335 (2002) 139–141.
[25] R. Welter, A.V. Morozkin, K. Halich, J. Magn. Magn. Mater. 257 (2003) 44–50.
[26] A.V. Morozkin, K. Halich, R. Welter, B. Ouladdiaf, J. Alloys Compd. 393 (2005) 34–40.
[27] G.M. Sheldrick, SHELXTL, Version 6.12, Bruker AXS Inc., Madison, WI, 2001.
[28] L.M. Gelato, E. Parthé, J. Appl. Crystallogr. 20 (1987) 139–143.
[29] P. Villars (Ed.), Pauling File Binaries Edition, Version 1.0, ASM International, Materials Park, OH, 2002.
[30] M.N. Abdusalyamova, N.A. Vlasov, Yu.M. Goryachev, Inorg. Mater. (Transl. Izv. Akad. Nauk SSSR, Neorg. Mater.) 20 (1984) 1242–1245.
[31] N.L. Eatough, H.T. Hall, Inorg. Chem. 8 (1969) 1439–1445.
[32] A. Kjekshus, F. Grønvold, J. Thorbjørnsen, Acta Chem. Scand. 16 (1962) 1493–1510.
[33] S. Derakhshan, A. Assoud, K.M. Kleinke, E. Dashjav, X. Qiu, S.J.L. Billinge, H. Kleinke, J. Am. Chem. Soc. 126 (2004) 8295–8302.
[34] R. Berger, Acta Chem. Scand. Ser. A: Phys. Inorg. Chem. 31 (1977) 889–890.
[35] J.W. Kaiser, M.G. Haase, W. Jeitschko, Z. Anorg. Allg. Chem. 627 (2001) 2369–2376.
[36] S. Bobev, H. Kleinke, Chem. Mater. 15 (2003) 3523–3529.
[37] M. Armbrüster, R. Cardoso Gil, U. Burkhardt, Yu. Grin, Z. Kristallogr.—New Cryst. Struct. 219 (2004) 209–210.
[38] H. Nowotny, R. Funk, J. Pesl, Monatsh. Chem. 82 (1951) 513–525.
[39] H. Auer-Welsbach, H. Nowotny, A. Kohl, Monatsh. Chem. 89 (1958) 154–159.
[40] Y. Zhu, H. Kleinke, Z. Anorg. Allg. Chem. 628 (2002) 2233.
[41] H. Kleinke, Inorg. Chem. 40 (2001) 95–100.
[42] H. Bie, A. Mar, Unpublished information.
[43] L. Pauling, The Nature of the Chemical Bond, third ed., Cornell University Press, Ithaca, NY, 1960.
[44] G.A. Papoian, R. Hoffmann, Angew. Chem. Int. Ed. 39 (2000) 2408–2448.
[45] W.B. Pearson, The Crystal Chemistry and Physics of Metals and Alloys, Wiley, New York, 1972.